

Magazine of Civil Engineering

ISSN 2712-8172

journal homepage: http://engstroy.spbstu.ru/

Research article

UDC 624.04

DOI: 10.34910/MCE.144.8

CC BY NC

Seismic influence of end shear walls in tall buildings with linker bridge systems

M.M. Sabri[1], ***M. Akhavan Salmassi***[2] ✉

[1] *Moscow Automobile and Road Construction State Technical University "MADI", Moscow, Russian Federation*

[2] *Islamic Azad University, Semnan Branch, Semnan, Iraq*

✉ *m.akhavansalmassi@iau.ir*

Keywords: tall buildings, nonlinear time history analysis, linker bridge, reinforced concrete structures, end shear walls.

Abstract. Contemporary architectural demands significantly influence structural analysis studies. In this regard, some tall buildings are linked by linker bridge to satisfy the functional demand. However, lateral loads significantly influence the seismic performance of such interconnected systems. This seismic load is a key consideration for structural designers working on tall buildings subjected to earthquake-induced forces. End shear walls in high-rise structures help alleviate stress concentrations caused by increased pressure at the extremities of the walls. In this study, nonlinear time history analysis was employed to compare the seismic effects of end shear walls in two 30-story buildings, one with and one without end shear walls connected by a steel linker bridge. The results showed that the average maximum absolute displacement decreased by 14 % under far-field ground motion records at the floor level where the linker bridge is located, specifically in the corner region adjacent to the bridge, in structures incorporating end-positioned shear walls. Additionally, the skewness coefficient of the acceleration record decreased by 65 % and 66 % due to the presence of end shear walls at the same floor level. In general, the two tall buildings equipped with connecting bridges and end shear walls showed notably better seismic effectiveness under earthquake loading. Previous investigations on linked tall buildings have studied parameters such as bridge location, stiffness, and end conditions, but the specific role of end shear walls within such interconnected systems remains unexplored. This study addresses this gap by investigating the seismic impact of end shear walls in two 30-story buildings connected by a steel linker bridge.

Funding: Ministry of Science and Higher Education of Russian Federation (funding No FSFM-2024-0025).

Citation: Sabri, M.M., Akhavan Salmassi, M. Seismic influence of end shear walls in tall buildings with linker bridge systems. Magazine of Civil Engineering. 2026. 19(4). Article no. 14408. DOI: 10.34910/MCE.144.8

1. Introduction

Tall buildings' seismic response is now a significant consideration for structural designers. Tall buildings can also be linked using liker bridges. Since reinforced concrete shear walls had high tensions at their flanges, the structural performance is obtained by connecting the end walls at all wall levels. Despite the growing use of linker bridges in tall building design, the seismic implications of end shear walls in such interconnected systems remain largely unexplored. While previous investigations have examined the behavior of isolated towers or generic coupling mechanisms, there is a noticeable lack of research on the effect of end shear walls and linker bridges in two high-rise configurations. The absence of detailed investigations into how end shear walls influence inter-tower dynamics, particularly at the floor level where

© Sabri, M.M., Akhavan Salmassi, M., 2026. Published by Peter the Great St. Petersburg Polytechnic University.

the bridge is located, underscores the need for targeted research in this area. This study addresses a critical gap in the literature by evaluating the seismic performance of two tower systems with end shear walls and linker bridge under far-field ground motion records. Despite the substantial body of research on linked tall buildings, a crucial review of the literature identifies several gaps. Previous studies have mainly investigated parameters such as bridge location, stiffness, connection types, and material properties, but the specific influence of end shear walls an essential structural element for lateral load resistance within linked tower systems remains largely unexamined [3–5, 10, 17]. While isolated towers with end shear walls have shown improved seismic behavior [1, 2, 6], and twin towers have been studied with various connection arrangements [8, 9, 11, 14], no study has systematically investigated the combined effect of end shear walls and linker bridges on the seismic performance of twin-tower systems. Furthermore, the interaction between end shear walls and the dynamic response at the crucial floor level where the linker bridge is situated has not been sufficiently addressed, especially regarding displacement control, acceleration distribution, and column force requirements [15, 16, 18]. This research gap is significant because end shear walls have the potential to substantially alter the load distribution mechanism and dynamic properties of interconnected towers, affecting both individual tower behavior and the overall system performance. This study studied the seismic consequences of two tall buildings, one with end shear walls and the other without using a linker bridge. Accordingly, the following were revealed by a few of the investigations.

Research focuses on the seismic and chaotic behavior of end shear walls. According to [1, 2], tall buildings equipped with end shear walls showed improved seismic behavior. According to a case study titled "Optimizing Seismic Design of Multi-Tower Buildings Using Sky Bridge Isolation and BIM," an isolation system at the sky bridge connection enhances torsional behavior [3]. This study shows the optimal sky-bridge location for coupled high-rise buildings using seismic vulnerability functions, investigating steel versus concrete materials and hinged versus fixed connections, and realize that steel-framed sky-bridges with hinged ends provide superior durability and extended resistance to ground motions in contrast to concrete alternatives with rigid connections [4].

Furthermore, the structural coupling-based seismic response analysis of linked twin-story tall buildings revealed findings from the investigation that the link might successfully alter the linked building system's structural reactions. In certain instances, the structural reactions have been reduced compared to a single tower. This is because the additional link stiffness acts as a seismic brace for the single tower. However, in certain instances, the reactions have been higher due to the increased mass of the link [5]. The seismic performance of shear walls as affected by regular and staggered openings: a thorough investigation revealed that considering the apertures during construction design is crucial since they significantly impact the seismic behavior of the shear wall. Nevertheless, shear wall behavior is slightly affected by the opening style regular or staggered [6]. The dynamic features and seismic response of RC buildings, as investigated by researchers, are highly sensitive to structural type and configuration, with characteristics such as building height, column orientation, and beam to column stiffness ratios fundamentally governing deformation patterns [7]. A suitable design strategy for the lateral stiffness of tall buildings made of steel and concrete was improved method, which is effective and practical by applying it to the initial layout of an 88-story Hong Kong building [8]. Research on the impact of connecting Bbeams in twin tower structures found that, according to some researchers [9], the maximum allowable "lateral sway" at the structure's peak due to wind can only be achieved if all floors are connected using connecting beams. Examining the horizontal vibration properties of a rigidly coupled building with twin towers of differing heights to find an appropriate position for the connecting body within the tower height, one can utilize numerical simulations and engineering examples to regulate and optimize the design scheme using simplified structural dynamics [10]. According to a review on seismic analysis of twin-tower structures optimal sky-bridge connections can reduce displacement responses by roughly 22 %, and the use of flexible connections between towers allows them to function as energy dissipation members during seismic events [11]. A review on structural dynamics under dynamic loads demonstrated that ANSYS excels in transient response, ABAQUS is remarkably reliable for severe conditions, and LS-DYNA is highly effective for impact scenarios offering engineers actionable guidance for software selection based on project requirements [12]. The researchers searched the seismic behavior of a legacy building with isotropic and orthotropic material properties through a comparative evaluation, and the results indicated that normal and shear stresses calculated from the models were verified against empirical relationships from the reference code of practice [13]. In conduct of multi-story twin structure connections of beams at different levels: a brief review, the researchers present the criteria for bridging the link between towers, including story displacement, story shear, and story drift, under seismic and wind circumstances [14]. Investigation of a tall twin tower taking a lateral load into account in light of I.S. 1893: I: 2016 and the use of ETABS revealed that division of the height of a level by the distance between two consecutive stories can lead to "story drift." Another term for the amount that a story moves due to lateral forces is story displacement. Important considerations for the design of curtain walls and partitions include story drift. There was a 1.9 % increase in story drift for the twin-connected structure compared to the twin structure in the center [15]. Examining the effects of seismic loading on twin and single towers by the use of electronic tabs revealed that there is

a 49.98 % increase at Story 80 compared to a single story in the case of twin tower shear in the x direction (EQ x) [16]. Seismic resilience, sustainability, and torsional performance of asymmetric twin-tower high-rise structures in seismic zone V demonstrated that controlled asymmetry, strategic sky bridge placement, and the use of sustainable materials can enhance both safety and environmental performance in high-rise buildings located in seismically active regions, providing valuable insights for designers and decision-makers [17]. The effect of using sky bridge and its various design methods on the performance of multi tower revealed that, for twin-tower structures, applying an energy-based performance design method for the sky bridge led to an average roof displacement reduction of 9.2 %, while the force-based method incorporating isolators and dampers resulted in a 7 % reduction [18].

The research object of this study is the seismic behavior of two 30-story reinforced concrete tall buildings connected by a steel linker bridge, with a particular focus on the influence of end shear walls on the structural response under far-field earthquake ground motions. The aim of this study is to examine and quantify the seismic effect of end shear walls on the dynamic performance of twin-tower high-rise buildings connected by a linker bridge, and to provide design guidelines for improving the seismic resilience of such interconnected systems. To achieve this aim, the following objectives are followed: (1) to develop nonlinear time history analysis models of two 30-story twin-tower arrangements one with end shear walls and one without using ETABS software, with both models connected by a steel linker bridge; (2) to evaluate and compare the seismic response parameters, including acceleration, displacement, and column forces, at critical locations (particularly at the floor level adjacent to the linker bridge) under three far-field ground motion records corresponding to low, medium, and high PGA/PGV ratios; (3) to statistically analyze the dynamic response data using skewness, kurtosis, box plots, and Q-Q plots to evaluate the regularity and dispersion of the structural behavior; and (4) to assess quantitatively the effectiveness of end shear walls in reducing seismic demands and improving structural stability, especially at the bridge connection level.

The study of the effect of end shear walls on the nonlinear behavior of two reinforced concrete buildings connected by linker bridge has been emphasized in previous literature. To address this research gap, the present study concentrates on two 30-story reinforced concrete towers connected by linker bridge; two towers have end shear walls, and the others do not. These buildings are analyzed under far-field seismic excitation. The novelty of this study lies in its integrated approach to evaluate the inter-tower dynamics, including displacement, column force, and acceleration at critical edge points, which are investigated using nonlinear time history analysis. Unlike previous studies that mainly investigated individual towers or overall connection systems, this study shows that end shear walls not only affect the seismic performance of individual tall buildings but also play an important role in maintaining the structural integrity and safety of the linker bridge. This dual focus provides a novel framework for optimizing seismic resilience in high-rise multi-tower configurations.

2. Material and Methods

2.1. Mathematical Formulation

Notation Summary

I_ω: Warping moment of inertia; J_1: Torsion constant; $B(z)$: Second moment; $\sigma(c,z)$: Vertical tension of the wall at a distance c from the neutral axis; $T_w(z)$: The torsion associated with the warping; $T_v(z)$: The torsion associated with the shear currents; $\sigma(s,z)$: The Distribution of tension in height (z); $\omega(s)$: Field coordinates; H: The height of the structure; A: The area of the plan; u: Poisson's coefficient; f_c: Concrete comprehensive strength; ρ: Concrete reinforced ratio; f_y: Yield strength of steel.

Torsion plays a pivotal role in the behavior of shear walls in tall buildings. These systems exhibit high rigidity at the base core, while torsional effects become pronounced toward the top. The shear walls are symmetrically aligned along both X and Y axes, modelled with a simplified I-shaped cross-section subjected to torsion with an eccentricity ratio of 0.05, revealing noticeable warping effects (ASCE 7-16, 2016 [18]). Under applied torsional moment T around the Z-axis, the wings and Z-axis rotate about the shear center, while the X-axis and vertical axis respond accordingly. Presently, slab sections rotate in opposing directions around the X-axis, and plate elements exhibit out-of-plane warping.

$$T_v(z) = GJ_1 \frac{d\theta}{dz}(z). \quad (1)$$

I_ω is the geometric property of the section and it called the warping moment of inertia or the warping constant. Also, J_1 is the torsion constant and the torsion equation resulting from the warping is as follows:

$$-EI_w \frac{d^3\theta}{dz^3}(z) + GJ_1 \frac{d\theta}{dz}(z) = T. \tag{2}$$

On the other hand, $B(z)$ is an action which is called the second moment:

$$B(z) = M(z)L. \tag{3}$$

$\sigma(c,z)$ is the vertical tension of the wall at a distance c from the neutral axis:

$$\sigma(c,z) = \frac{M(z)c}{I}. \tag{4}$$

For the rigid warping effect of the uniform cores under the influence of the torsion, we can refer to the theory of Vlasov. In order to study the differential equation, we can assume a core that is rigid at the bottom and free at the top and is under the influence of the extensive torsion $m(z)$. For the analysis of the equation, we can assume that the core has a cross section with uniform dimensions and properties at all altitudes.

The general warping is defined as:

$$T(z) = T_v(z) + T_w(z). \tag{5}$$

The torsion associated with the warping is defined as:

$$T_w(z) = -EI_\omega \frac{d^3\theta}{dz^3}(z). \tag{6}$$

And the torsion associated with the shear currents is as follows:

$$T_v(z) = GJ \frac{d\theta}{dz}(z). \tag{7}$$

The differential equation representing the torsion of the warping of the core is as follows:

$$\frac{d^4\theta}{dz^4}(z) - \alpha^2 \frac{d^2\theta}{dz^2}(z) = \frac{m(z)}{EI_\omega}. \tag{8}$$

In which:

$$\alpha^2 = \frac{GJ}{EI_\omega}. \tag{9}$$

In a uniform extensive torsion by applying boundary conditions, we will have:

$$\theta(z) = \frac{mH}{EI_\omega}\left\{\frac{1}{(\alpha H)^4}\left[\frac{(\alpha H \sin h\,\alpha H + 1)}{\cos h\,\alpha H}(\cos h\,\alpha z - 1) - \right.\right.$$
$$\left.\left. - \alpha H \sin h\,\alpha z + (\alpha H)^2\left[\frac{z}{H} - \frac{1}{2}\left(\frac{z}{H}\right)^2\right]\right]\right\}; \tag{10}$$

$$\alpha H = H\sqrt{\frac{GI}{EI_\omega}}; \tag{11}$$

$$\alpha z = \alpha H\left(\frac{z}{H}\right). \tag{12}$$

The above equation consists of two independent parts. The parts inside the brackets represents the distribution of rotation in the height, and it is a function of dimensionless structures parameters of αH and Z/H.

On the other hand, mentioned the warping stresses are calculated as follows with respect to the second moment $B(z)$.

$$B(z) = -EI_{\omega}\frac{d^2\theta}{dz^2}(z); \tag{13}$$

$$\sigma(s,z) = \frac{B(z)\omega(s)}{I_{\omega}}. \tag{14}$$

As it can be seen in Equation (14), adding an end wall reduces the stresses and consequently reduces the effect of warping and torsion.

Based on the referenced equations, particularly Equation (14) and the observed reduction in stress due to the presence of end shear walls, the enhancement of key parameters reflects their effective structural performance.

2.2. The Specification of the Structures

In this study, two 30-story buildings with linker bridges were modeled in two types, with end shear walls and without them. Also, the ETABS [19] software is considered to analyze the buildings mentioned above. The study focused on constructions incorporating moment frames and shear wall configurations made of reinforced concrete. The applied dead load was 170 kg/m^2, while the live load was 200 kg/m^2. The shear walls and column connections were fixed at the base, with RC slabs as floors. The study accounted for dead and live loads of 170 kg/m^2 and 200 kg/m^2, respectively, along with a concrete compressive strength (f_c) of 50 MPa, Poisson's ratio (u) of 0.15, and steel yield strength (f_y) of 400 N/mm^2. Both models adhered to the ASCE7-16 [18] code. Also, the linker bridge considered steel structures and reinforced concrete slabs. On the other hand, the aforementioned bridge is connected by joint support to T1 towers and roller support to T2 towers, respectively (Fig. 2a and Fig. 2c). After the frames were categorized in three dimensions using the ETABS software, the portions of the frames were determined. The end shear walls are in blue in Figs. 1b and 1c and red in Fig. 1a.

The nonlinear time-history analysis was conducted using ETABS [19]. To precisely capture the inelastic behavior of the structures under seismic loading, plastic hinges were designated at the ends of frame elements. For beams, M3 (moment) hinges were specified, while for columns, P-M2-M3 (interaction) hinges were employed to account for axial force-bending moment interaction. All frame elements were modeled using beam-column elements with nonlinearity at hinge locations, while the concrete shear walls were modeled using multi-layer shell elements with a fine mesh to ensure adequate accuracy in stress distribution.

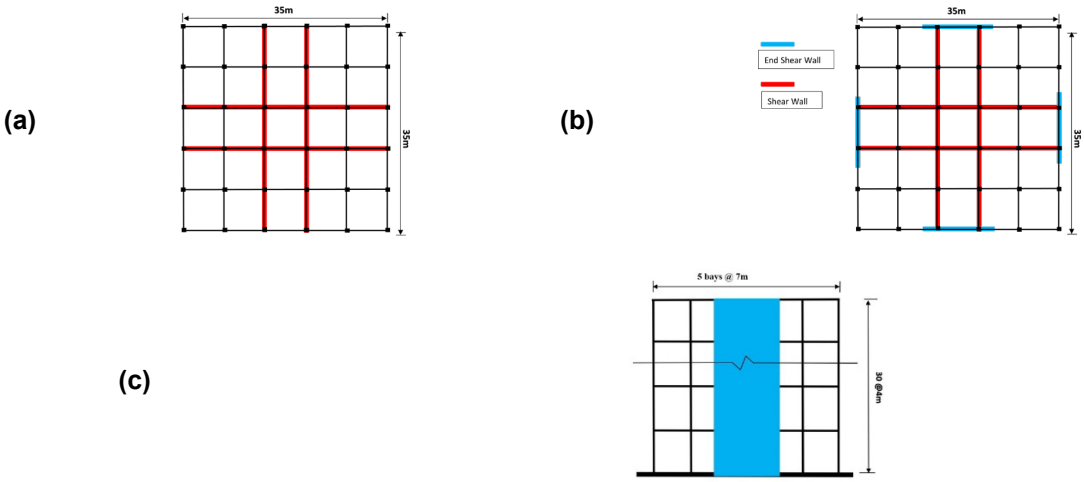


Figure 1. 30-story structural models: (a) Floor plan of the 30-story building without end shear walls; (b) Floor plan of the 30-story building incorporating end shear walls; (c) Elevation view of the 30-story high-rise structure featuring end shear walls.

On the other hand, Figs. 2a and 2b indicate the arrangement of the tall buildings by linker bridges without and with end shear walls. The mentioned structures are modeled using ETABS software for nonlinear time history analysis. In this regard, some edge points are considered for further investigations: two points in the corners plans of CMF1T1 and CMF1T2, and two points in the intersections of the plans and linker bridges (A, B, C, and D) at 23 level. Also, the abovementioned points are considered for CMF2T1 and CMF2T2, too (E, F, G, and H). These points are intended to investigate the effect of end shear walls in two tall buildings connected by a linker bridge.

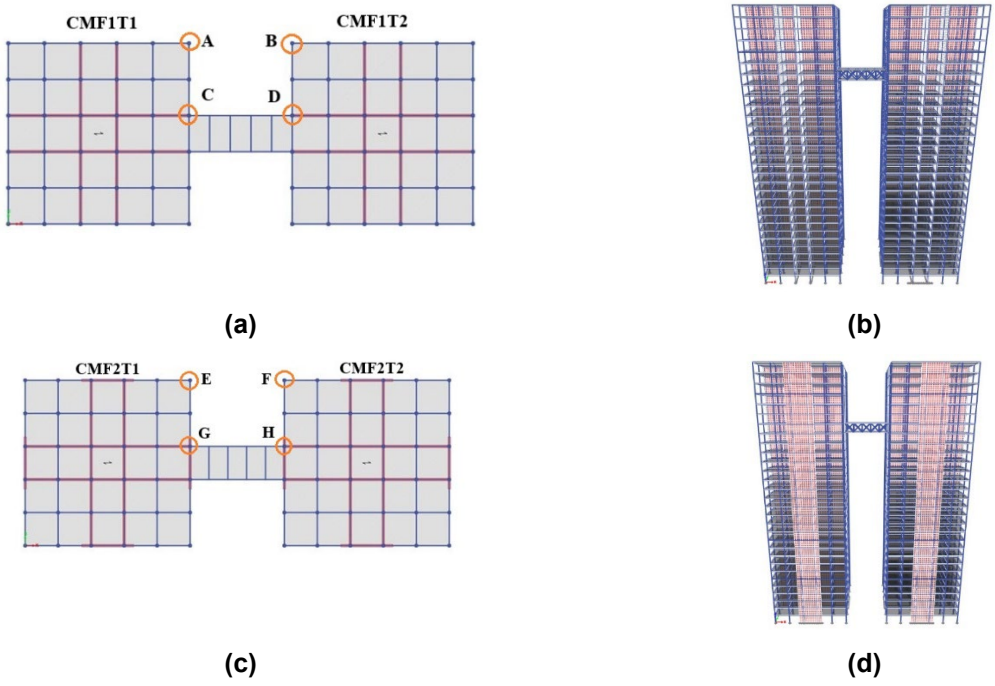


Figure 2. 30-story two-tall buildings by linker bridge models: (a) Twin Towers plan by linker bridge without end shear wall; (b) Twin Towers 3-dimensions by linker bridge without end shear wall; (c) Twin Towers plan by linker bridge with end shear wall; (d) Twin Towers 3-dimensions by linker bridge with End shear wall.

Table 1 shows the buildings' specifications and the height, area, and dimensions. Table 2 also indicates the section size.

Table 1. Case Specifications.

Label		No. of Story	H (m)	A (m^2)	Plan Dimensions (m×m)
CMF1T1	Without end shear wall – Tower1	30	120	36750	35×35
CMF1T2	Without end shear wall – Tower2	30	120	36750	35×35
CMF2T1	With end shear wall – Tower1	30	120	36750	35×35
CMF2T2	With end shear wall – Tower2	30	120	36750	35×35

Table 2. Size of Sections.

Item	Element	Rebar	Dimension
T1, T2	Column	36Φ32 – Stirrup Φ14@15	Story 1–15: (1.20) m × (1.20) m Story 16–30: (1.00) m × (1.00) m
	Beam	8Φ20- Stirrup Φ14@10	Story 1–30: (0.5) m wide × (0.7) m deep
	Shear Wall	Φ28@10 - Stirrup Φ14@25	Story 1–30: (35) m long × (0.5) m thick
	End shear wall	Φ28@10 - Stirrup Φ14@25	Story 1–30: (11) m long × (0.5) m thick
	Slab	Φ10@10	Story 1–30: (0.15) m thick
Linker Bridge	Steel Braced	BOX 700*70	
	Steel Column	IPE550	
	Steel Beam	IPE 750*222	
	Slab	Φ10@10	Story 1–30: (0.15) m thick

Seismic analysis was performed on these structures following the modeling process, as indicated in the graphs.

Table 3 presents the record specifications, including site class D and far-field conditions. In parallel, Figs. 3a, 3b, and 3c show the acceleration time and the related response. Also, Fig. 4 shows the response acceleration-time of three far-field records, the seism signal software [21] used for graphs as mentioned above.

The records are chosen using the PGV/PGA ratio, defined as the maximum ground acceleration divided by the maximum ground velocity [20]. According to this theory, low-speed cycles are caused by stone buildings' high PGA but short duration. The ratio of PGA to PGV is high in these records.

Regarding structural responses, stiffer structures require high PGA/PGV records. Concurrently, under PGA/PGV records, the shocks are more severe for the highly flexible structures. The following boundaries characterize the predicted spectrum of PGA/PGV ratios [20].

Low: PGA/PGV < 0.8;

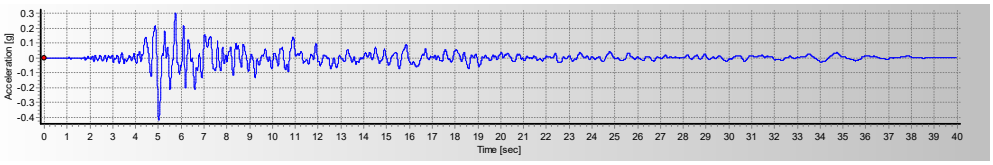
Medium: 0.8 <PGA/PGV < 1.2;

High: 1.2 <PGA/PGV.

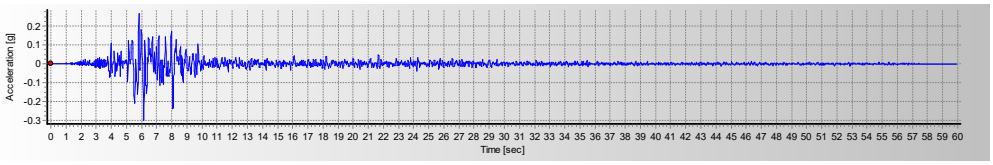
Three examples were chosen for certainty based on the data in Table 3, which includes high, medium, and low cases.

Table 3. Far-field earthquake records used in the analysis.

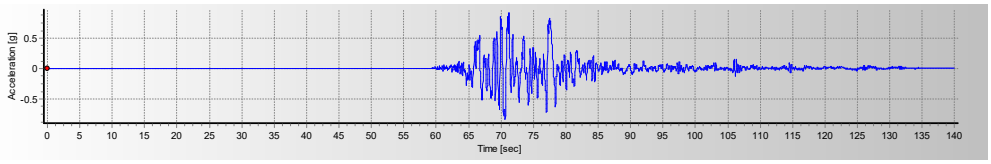
Record	Event	Station	PGA (g) / PGV (m/sec)	PGA (g)	Magnitude (Richter)	Earthquake depth (km)	Year
R1	Loma Prieta	Gilroy Array #4	1.04	0.419	6.93	14.34	1989
R2	Northwest China-03	Jaishi	1.56	0.3	6.1	17.73	1997
R3	Chuetsu-Oki	Kashiwazaki NPP_Unit1: ground surface	0.66	0.9	6.8	11.00	2007



(a) Loma Prieta (R1)



(b) Northwest China-03 (R2)



(c) Chuetsu-Oki (R3)

Figure 3. Acceleration vs time graphs for three far-field earthquake records: (a) Loma Prieta, acceleration-time; (b) Northwest China-03, acceleration-time; (c) Chuetsu-Oki, acceleration-time.

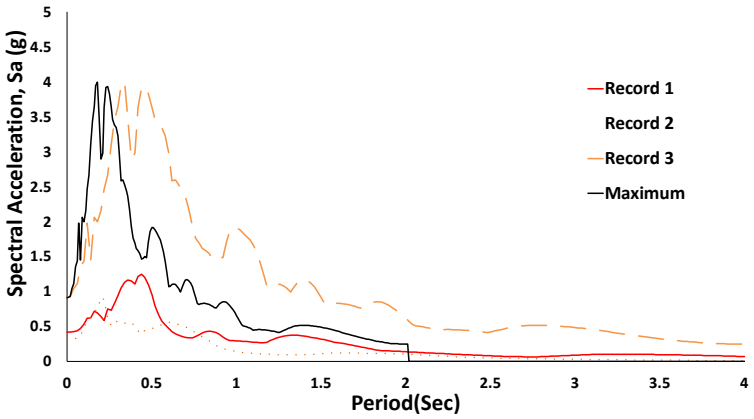
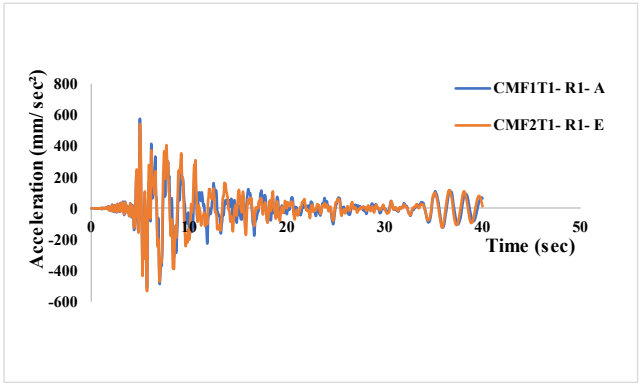


Figure 4. The spectral response of records.

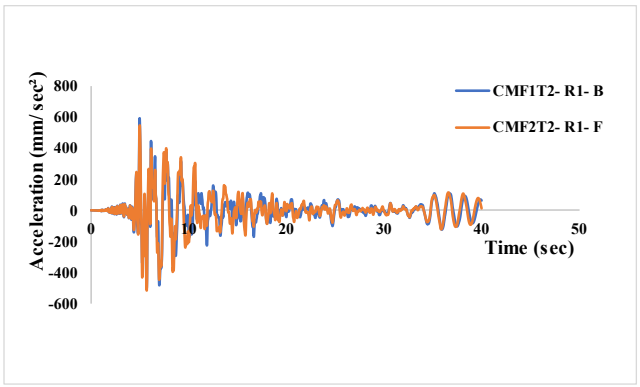
3. *Results*

The ETABS software was used to simulate two 30-story buildings in accordance with the ASCE7-16 code. Additionally, a steel bridge linker connects the two tall buildings. The structures indicated were exposed to three far-field records. Additionally, specific investigations utilized nonlinear time history analysis.

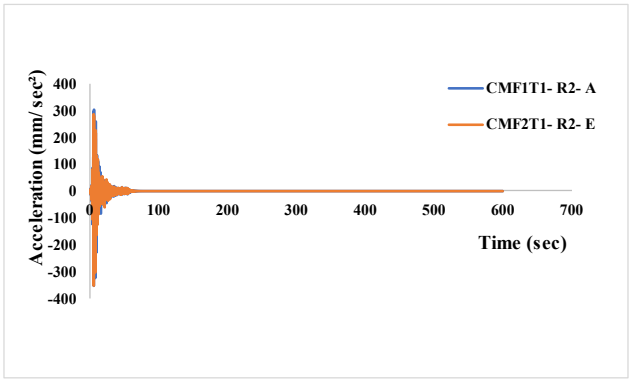
On the other hand, acceleration is a key parameter affecting occupant comfort in tall buildings. In this regard, acceleration versus time was analyzed at Level 23 to evaluate this parameter. Fig. 5a to Fig. 5f present the acceleration versus time responses for CMF1T1, CMF1T2, CMF2T1, and CMF2T2 tall building configurations subjected to R1 to R3. All cases indicate a reduction in acceleration at Level 23 due to the implementation of end shear walls. This emphasizes that the two tall buildings incorporating linker bridges with end shear walls exhibit increased seismic performance. This reduction in acceleration shows a more controlled dynamic environment, which not only improves comfort for occupants but also declines vibrational stress on the linker bridge. Lower acceleration levels help prevent fatigue, resonance, and potential damage to bridge connections, thereby increasing the overall seismic resilience of the two high-rise system.


CMF1T1- R1- A
CMF2T1- R1- E
Acceleration (mm/ sec²)
800
600
400
200
0
-200
-400
-600
0
10
20
30
40
50
Time (sec)

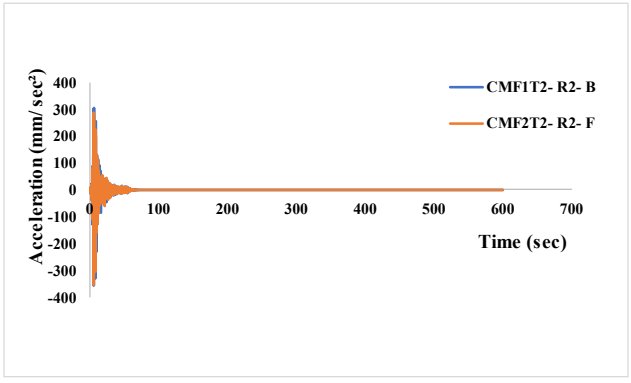
(a)


CMF1T2- R1- B
CMF2T2- R1- F
Acceleration (mm/ sec²)
800
600
400
200
0
-200
-400
-600
0
10
20
30
40
50
Time (sec)

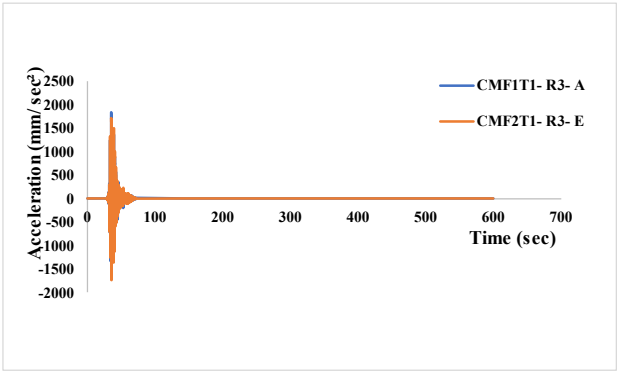
(b)


CMF1T1- R2- A
CMF2T1- R2- E
Acceleration (mm/ sec²)
400
300
200
100
0
-100
-200
-300
-400
0
100
200
300
400
500
600
700
Time (sec)

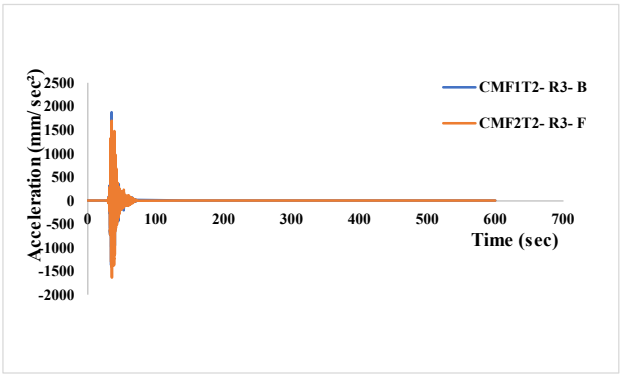
(c)


CMF1T2- R2- B
CMF2T2- R2- F
Acceleration (mm/ sec²)
400
300
200
100
0
-100
-200
-300
-400
0
100
200
300
400
500
600
700
Time (sec)

(d)



(e)



(f)

Figure 5. Acceleration versus time in CMF1T1, CMF1T2, CMF2T1, and CMF2T2 tall buildings at A, B, E, and F points subjected to three records: (a) Acceleration versus time in CMF1T1, CMF2T1 tall buildings at A and E subjected to R1; (b) Acceleration versus time in CMF1T2, CMF2T2 tall buildings at B and F subjected to R1; (c) Acceleration versus time in CMF1T1, CMF2T1 tall buildings at A and E subjected to R2; (d) Acceleration versus time in CMF1T2, CMF2T2 tall buildings at B and F subjected to R2; (e) Acceleration versus time in CMF1T1, CMF2T1 tall buildings at A and E subjected to R3; (f) Acceleration versus time in CMF1T2, CMF2T2 tall buildings at B and F subjected to R3.

Table 4 presents the maximum absolute acceleration values for the CMF1T1, CMF1T2, CMF2T1, and CMF2T2 tall buildings subjected to three ground motion records. The results indicate that the incorporation of end shear walls significantly declines the maximum absolute acceleration. This suggests that the two tall buildings, including a linker bridge with end shear walls, display improved seismic performance. Furthermore, the average maximum absolute acceleration across the three records was compared for the mentioned arrangements. The average values for CMF1T1 and CMF1T2 were 1834.600 mm/sec^2 and 1873.095 mm/sec^2, respectively, while CMF2T1 and CMF2T2 recorded lower averages of 1738.988 mm/sec^2 and 1691.773 mm/sec^2. These results show the increased seismic response of the tall buildings with a linker bridge and end shear walls. Fig. 6 indicates the bar chart of maximum absolute acceleration for the CMF1T1, CMF1T2, CMF2T1, and CMF2T2 tall buildings subjected to three seismic records. This figure presents the improved comfort levels achieved in tall buildings that incorporate a linker bridge with end shear walls, according to the reduction in acceleration responses.

Table 4. The maximum absolute acceleration in CMF1T1, CMF1T2, CMF2T1, and CMF2T2 tall buildings is subjected to three records.

Item	Maximum Absolute Acceleration (mm/sec^2)– CMF1T1–A	Maximum Absolute Acceleration (mm/sec^2)– CMF1T2–B	Maximum Absolute Acceleration (mm/sec^2)– CMF2T1–E	Maximum Absolute Acceleration (mm/sec^2)– CMF2T2–F
R1	574.589	592.1849	541.1148	546.3022
R2	352.2758	355.6708	351.9721	352.869
R3	1834.600	1873.095	1738.988	1691.773
Maximum	1834.600	1873.095	1738.988	1691.773

For further analysis, Fig. 6 shows the bar chart of the absolute maximum acceleration at points A, B, E, and F, respectively, in the tall buildings CMF1T1, CMF1T2, CMF2T1, and CMF2T2, which were subjected to three earthquake records (R1, R2, and R3). In this figure, the acceleration values at points E and F, which correspond to buildings with end shear walls, are lower than those at points A and B, which represent buildings without end shear walls. This reduction in maximum acceleration highlights the improved seismic performance of two tall buildings connected by a connecting bridge when end shear walls are used.

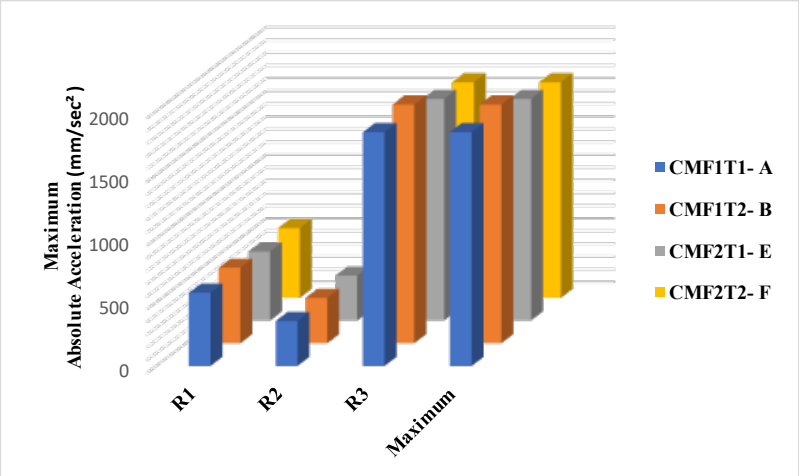


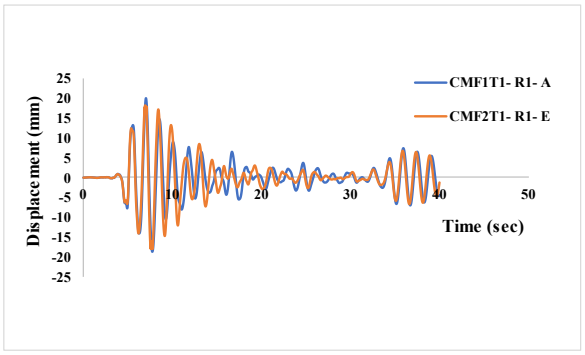
Figure 6. Bar chart of the maximum absolute acceleration at points A, B, E, and F in the CMF1T1, CMF1T2, CMF2T1, and CMF2T2 tall buildings, respectively, subjected to three seismic records (R1, R2, and R3).

According to Table 4, the maximum values are associated with R3. For further statistical analysis, IBM SPSS Statistics software [21] was used, and Table 5 presents the skewness and kurtosis coefficients of the maximum absolute acceleration in the CMF1T1, CMF1T2, CMF2T1, and CMF2T2 tall buildings subjected to R3. The skewness value of CMF2T1–R3–E is closer to zero than that of CMF1T1–R3–A, indicating a more symmetrical distribution. Similarly, the skewness coefficient of CMF2T2–R3–F is closer to zero than CMF1T2–R3–B. Furthermore, the kurtosis value of CMF2T1–R3–E is also closer to zero than CMF1T1–R3–A, and the kurtosis coefficient of CMF2T2–R3–F is more normalized compared to CMF1T2–R3–B. These results suggest that the acceleration data in the two tall buildings with end shear walls reveal less statistical dispersion than those without end shear walls. This reason the two tall buildings with end shear walls had better performance than the other two tall buildings. This result shows that the two tall buildings with end shear walls exhibited better seismic performance than the other two tall buildings.

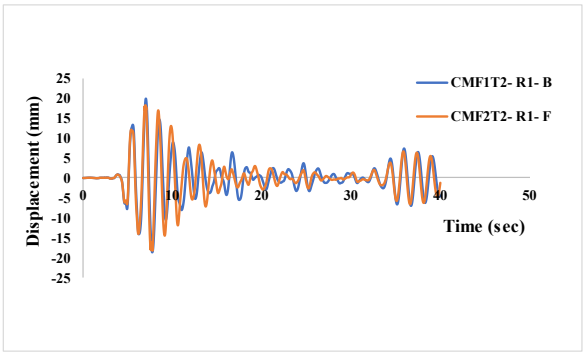
Table 5. The skewness and kurtosis coefficient of the maximum absolute acceleration in CMF1T1, CMF1T2, CMF2T1, and CMF2T2 tall buildings are subjected to R3.

Item	CMF1T1–R3–A	CMF2T1–R3–E	CMF1T2–R3–B	CMF2T2–R3–F
Skewness Coefficient	1.135	0.395	1.097	0.372
Kurtosis Coefficient	18.790	16.106	18.462	15.648

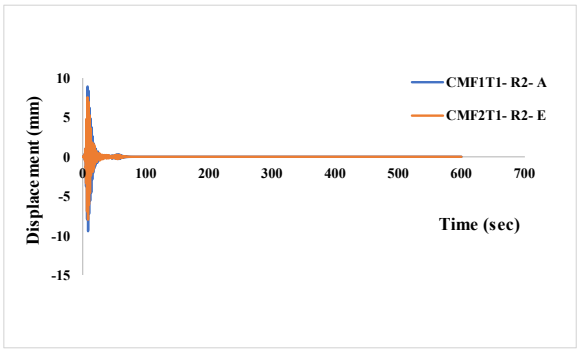
Fig. 7a to Fig. 7f present the displacement versus time responses at points A, B, E, and F in the CMF1T1, CMF1T2, CMF2T1, and CMF2T2 tall buildings, respectively, subjected to the three seismic records (R1, R2, and R3). This figure is essential for interpreting the dynamic behavior and time-dependent deformation patterns of structures. By comparing the displacement history at corresponding points of buildings with and without end shear walls, it is shown how the structural arrangement affects lateral motion, energy dissipation, and peak response. The time-domain analysis also helps to identify possible resonance effects and phase shifts between connected towers and provides valuable insight into the effectiveness of end shear walls in controlling inter-story drift and increasing seismic resilience. Importantly, the maximum displacements under all three earthquake records are reduced in the two tall buildings equipped with connecting bridges and end shear walls. This suggests that the presence of end shear walls improves the seismic performance of the connected towers, especially at Level 23, where the linker bridge is located and dynamic interaction is most critical.


CMF1T1- R1- A
CMF2T1- R1- E
Displacement (mm)
Time (sec)

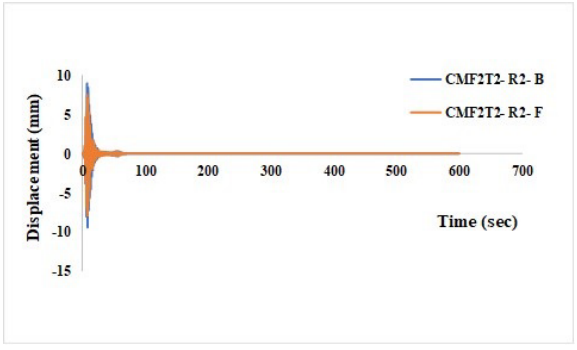
(a)


CMF1T2- R1- B
CMF2T2- R1- F
Displacement (mm)
Time (sec)

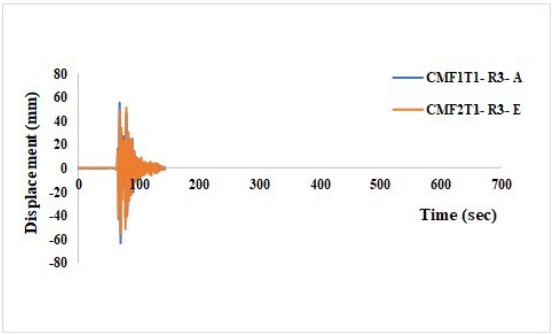
(b)


CMF1T1- R2- A
CMF2T1- R2- E
Displacement (mm)
Time (sec)

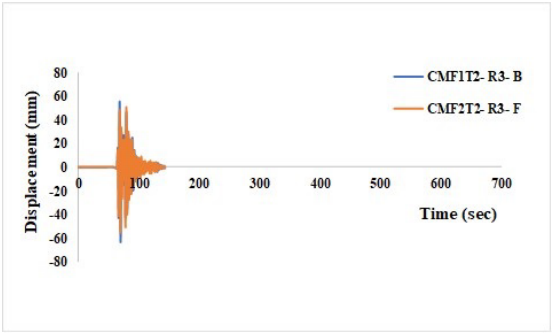
(c)


CMF2T2- R2- B
CMF2T2- R2- F
Displacement (mm)
Time (sec)

(d)



(e)



(f)

Figure 7. Displacement versus time in CMF1T1, CMF1T2, CMF2T1, and CMF2T2 tall buildings at A, B, E, and F points subjected to three records: (a) Displacement versus time in CMF1T1, CMF2T1 tall buildings at A and E subjected to R1; (b) Displacement versus time in CMF1T2, CMF2T2 tall buildings at B and F subjected to R1; (c) Displacement versus time in CMF1T1, CMF2T1 tall buildings at A and E subjected to R2; (d) Displacement versus time in CMF1T2, CMF2T2 tall buildings at B and F subjected to R2; (e) Displacement versus time in CMF1T1, CMF2T1 tall buildings at A and E subjected to R3; (f) Displacement versus time in CMF1T2, CMF2T2 tall buildings at B and F subjected to R3.

For extended inquiry, Table 6 presents the maximum absolute displacement values at points A, B, E, and F in the CMF1T1, CMF1T2, CMF2T1, and CMF2T2 tall buildings, respectively, under three seismic records. The displacement values at points E and F are notably lower than those at points A and B. Specifically, the maximum absolute displacement at CMF1T1–A decreased from 63.36321 mm to 55.32871 mm in CMF2T1–E, and at CMF1T2–B it declined from 63.36879 mm to 54.758931 mm in CMF2T2–F. These reductions show that the integration of end shear walls significantly improved the seismic performance of the two tall buildings connected by a linker bridge, especially in controlling lateral displacement.

Table 6. The maximum absolute displacement in CMF1T1–A, CMF1T2–B, CMF2T1–E, and CMF2T2–F tall buildings are subjected to three records.

Item	Maximum Absolute Displacement (mm)–CMF1T1–A	Maximum Absolute Displacement (mm)–CMF1T2–B	Maximum Absolute Displacement (mm)–CMF2T1–E	Maximum Absolute Displacement (mm)–CMF2T2–F
R1	19.96076	18.18159	19.88653	18.23236
R2	9.429619	9.410256	7.967806	7.7989
R3	63.36321	63.36879	55.32871	54.75893
Maximum	63.36321	63.36879	55.32871	54.75893

For further investigation, Fig. 8 shows the bar graph of the absolute maximum displacement at points A, B, E, and F in the tall buildings CMF1T1, CMF1T2, CMF2T1, and CMF2T2, respectively, subjected to three earthquake records (R1, R2, and R3). In this figure, the displacement values at point E and the buildings with end shear walls are less than those at points A and B, which represent buildings without end shear walls. This reduction in maximum displacement highlights the improved seismic performance of the two tall buildings connected by the linker bridge when end shear walls are used.

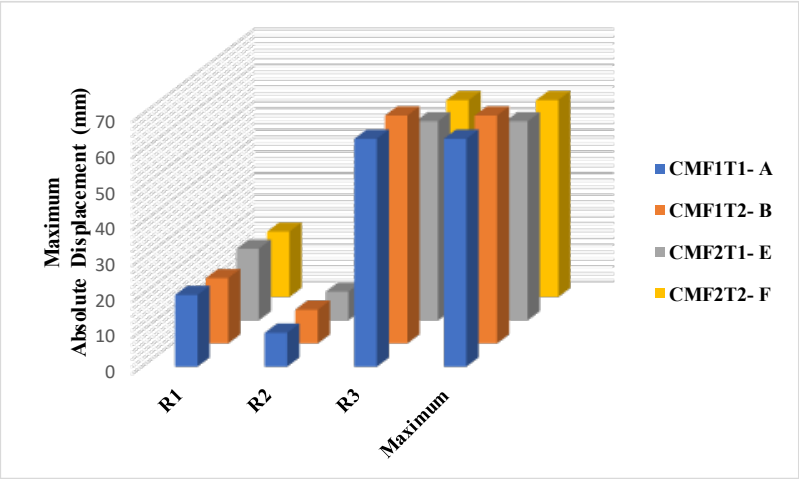


Figure 8. Bar chart of absolute maximum displacement at points A, B, E, and F, respectively, in tall buildings CMF1T1, CMF1T2, CMF2T1, and CMF2T2 subjected to three earthquake records (R1, R2, and R3).

Table 6 shows that the maximum absolute displacement in the tall buildings CMF1T1–A, CMF1T2–B, CMF2T1–E, and CMF2T2–F subjected to three earthquake records reached its maximum value in the R3 record. This showes that the R3 record had the most significant impact on the displacement among all four structural configurations.

In this regard, in order to investigate more accurately through statistical analysis, Fig. 9 shows the boxplot diagram of the maximum absolute displacement at points A, B, E, and F in the tall buildings CMF1T1, CMF1T2, CMF2T1, and CMF2T2 under the R3 seismic record, respectively. This figure provides a clearer view of the distribution, dispersion, and comparative performance of each structural system under the most critical loading conditions.

As can be seen, the boxplot variation range for CMF1T1–R3–A and CMF1T2–R3–B extends from approximately –65 mm to +60 mm, while the range for CMF2T1–R3–E and CMF2T2–R3–F is narrower, ranging from –60 mm to +50 mm. This reduction in displacement amplitude indicates that the buildings with end shear walls (CMF2T1 and CMF2T2) experienced less lateral oscillations under the R3 seismic record. This narrower range indicates better control over structural deformation and suggests that the use of end shear walls increases the seismic stability and resilience of the connected towers, especially in limiting the severe displacement responses.

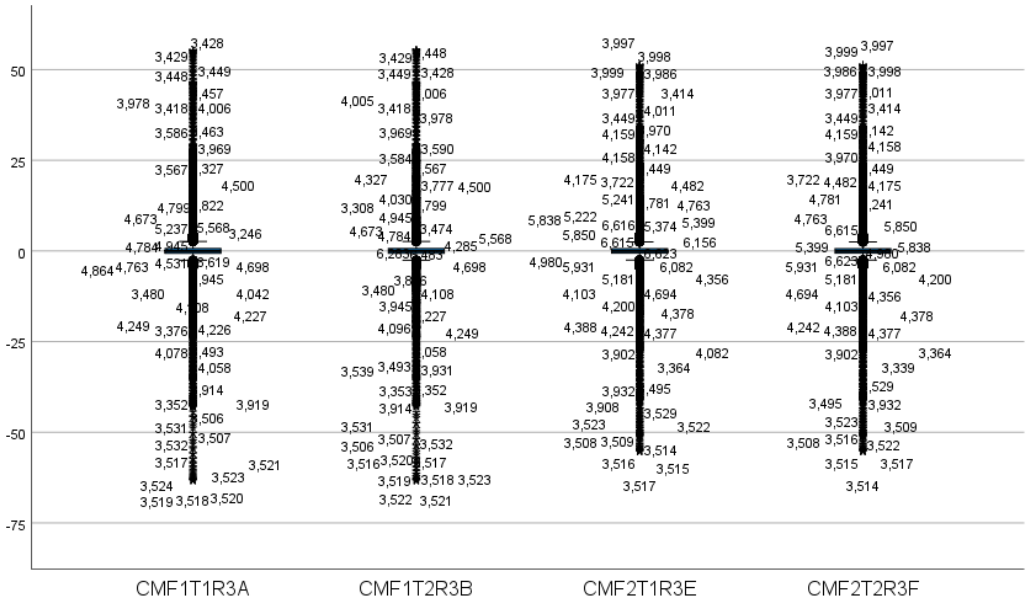


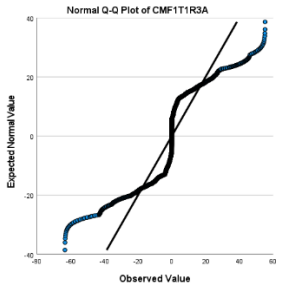
Figure 9. Boxplot of the maximum absolute displacement at points A, B, E, and F in the CMF1T1, CMF1T2, CMF2T1, and CMF2T2 tall buildings, respectively, subjected to seismic record (R3).

In continuation, Fig. 10 presents quantile–quantile (Q–Q) plots of the maximum absolute displacement at points A, B, E, and F in the CMF1T1, CMF1T2, CMF2T1, and CMF2T2 tall buildings, respectively, subjected to seismic record R3.

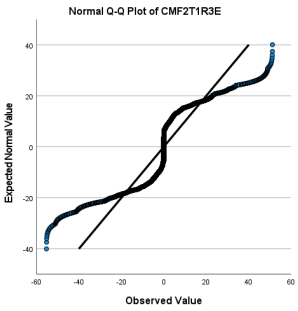
Figs. 10a and 10b present the normal Q–Q plots for CMF1T1–R3 at point A and CMF2T1–R3 at point E, respectively. The displacement values at point A are distributed across a wider range, approximately –60 mm to +60 mm, whereas the values at point E fall within a narrower range, indicating less variability in the CMF2T1–R3 dataset.

Fig. 10c displays the detrended normal Q–Q plot for CMF1T1–R3 at point A, revealing deviations from normality within the –30 mm to +20 mm domain. In contrast, Fig. 10d shows the detrended Q–Q plot for CMF2T1–R3 at point E, where deviations are more confined, within the –20 mm to +20 mm range. This suggests that the displacement distribution in CMF2T1 is more consistent with a normal pattern, reflecting improved structural regularity due to the presence of end shear walls.

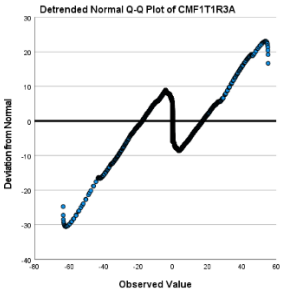
Similar conditions are observed in Figs. 10e and 10f for points B and F, respectively, with CMF2T2–R3 at point F showing a narrower deviation band compared to CMF1T2–R3 at point B. These comparisons further emphasize the stabilizing effect of end shear walls in reducing displacement irregularities under seismic loading.



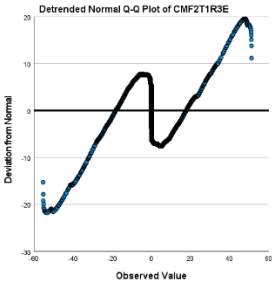
(a)



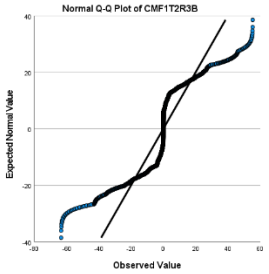
(b)



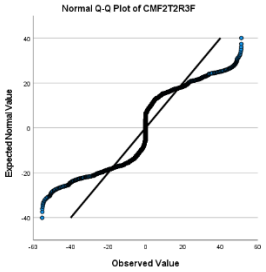
(c)



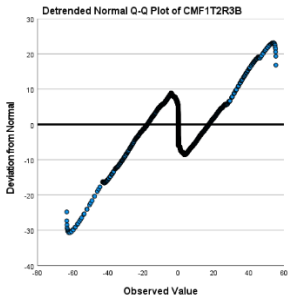
(d)



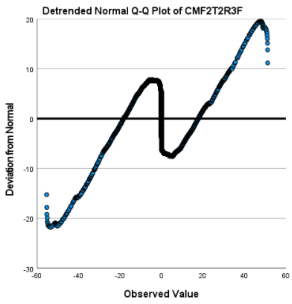
(e)



(f)



(g)



(h)

Figure 10. Q–Q plots of the maximum absolute displacement at points A, B, E, and F in the CMF1T1, CMF1T2, CMF2T1, and CMF2T2 tall buildings, respectively, subjected to seismic record R3: (a) Normal Q–Q plot for CMF1T1–R3 at point A; (b) Normal Q–Q plot for CMF2T1–R3 at point E; (c) Detrended normal Q–Q plot for CMF1T1–R3 at point A; (d) Detrended normal Q–Q plot for CMF2T1–R3 at point E; (e) Normal Q–Q plot for CMF1T1–R3 at point B; (f) Normal Q–Q plot for CMF2T1–R3 at point F; (g) Detrended normal Q–Q plot for CMF1T1–R3 at point B; (h) Detrended normal Q–Q plot for CMF2T1–R3 at point F.

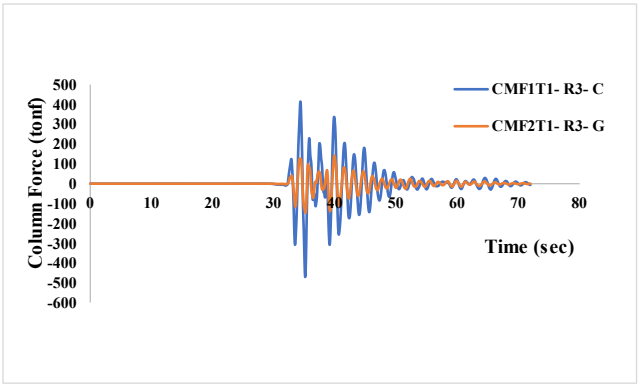
On the other hand, considering the dominant influence of seismic record R3 on structural behavior, Fig. 11 illustrates the column force versus time at points C, D, G, and H in the CMF1T1, CMF1T2, CMF2T1, and CMF2T2 tall buildings, respectively, subjected to R3.

Fig. 11a presents the column force response at points C and G in the CMF1T1 and CMF2T1 buildings. As shown, the force values at point G (CMF2T1–R3) are notably lower than those at point C (CMF1T1–R3). Specifically, the maximum column force is reduced from 469.9891 tonf to 146.6881 tonf due to the incorporation of end shear walls.

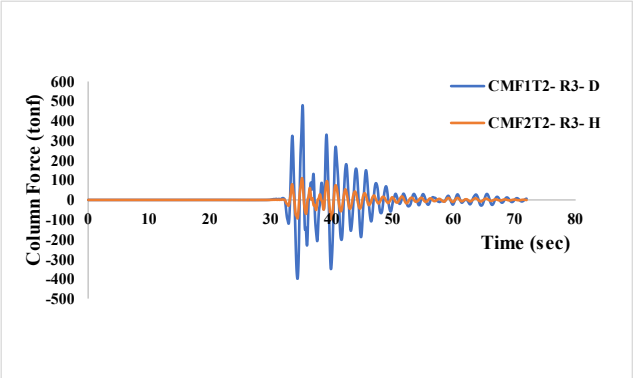
Fig. 11b shows the column force response at points D and H in the CMF1T2 and CMF2T2 buildings, respectively. A similar trend is observed, with the maximum column force decreasing from 478.8082 tonf at point D to 110.0862 tonf at point H, again demonstrating the effectiveness of end shear walls in reducing seismic force demands.

Column force is a crucial parameter in seismic analysis because it directly represents the changes in axial load acting on the vertical members of a structure during ground motion. Extreme increase in column force can lead to instability, buckling, or failure, especially in high-rise systems.

By analyzing column force over time, engineers will be able to evaluate dynamic load transfer, identify critical stress points, and investigate the effectiveness of seismic damage mitigation strategies such as the use of end shear walls and bridge abutments in increasing structural resilience.



(a)



(b)

Figure 11. Column force versus time at points C, D, G, and H, respectively, in tall buildings CMF1T1, CMF1T2, CMF2T1, and CMF2T2 subjected to the R3 seismic record: (a) Column force versus time at points C and G, respectively, in tall buildings CMF1T1 and CMF2T1 under the R3 seismic record; (b) Column force versus time at points D and H, respectively, in tall buildings CMF1T2 and CMF2T2 under the R3 seismic record.

Overall, the comparative results in displacement, acceleration, and column force indices consistently demonstrate the superior seismic performance of the CMF2T1 and CMF2T2 configurations, especially under the R3 seismic record. The integration of end shear walls and connecting bridges has resulted in a significant reduction in structural demands and improved displacement uniformity, which is clearly evident through statistical plots and nonlinear time history analyses. These findings provide a solid foundation for a deeper explanation and investigation of design implications, which will be discussed in the subsequent discussion section.

4. Discussion

The results of this study confirm that the use of end shear walls in twin-tower buildings connected by a connecting bridge substantially enhances the seismic response of the structure. Nonlinear time history analysis showed reductions in the absolute maximum acceleration, displacement, column force, and statistical dispersion, especially at the story adjacent to the connecting bridge where the dynamic interaction is more critical.

Similarly, others investigated lateral displacement and drift in twin towers with connecting beams and noted that the inter-tower connection can either intensify or reduce seismic effects depending on the stiffness and mass [4]. The present study complements this view and shows that end shear walls not only reduce drift but also smoothen the acceleration distribution, with a 65–66 % reduction in skewness and 14–15 % in kurtosis.

Some researchers investigated flyover isolation systems to improve torsional behavior. While their approach focused on isolation mechanisms, the present study demonstrates that appropriately placed end shear walls can provide similar improvements in torsional control and inter-tower stability, without the need for complex isolation equipment [3].

Also, the effectiveness of end shear walls in mitigating stress concentrations is corroborated by Vlasov's theory. As demonstrated by the model verification study (The results and Table 5), the analytical stress distribution predicted by Equation (14) aligns closely with the ETABS results. Consequently, the observed reduction in stress at the critical 23rd floor level, where the linker bridge is located, is fully consistent with the theoretical framework. This integration of theory and numerical evidence underscores the structural contribution of end shear walls in enhancing seismic performance.

This paper introduces a configuration that has rarely been investigated in previous studies: two 30-story reinforced concrete towers connected by a steel bridge, with and without end shear walls. Unlike previous studies that have mainly investigated individual towers or overall connection systems, this study provides a detailed statistical and dynamic assessment of the effect of end shear walls on seismic behavior at critical edge locations. Combining nonlinear time history analysis with statistical indices such as skewness, elongation, and Q–Q plots provides a comprehensive framework for assessing seismic resilience. These insights are critical for optimizing the design of multi-tower high-rise systems in seismic zones, especially where architectural requirements require interconnection between towers.

5. Conclusion

Two 30-story tall buildings modeled by ETABS software. Also, the two tall buildings are connected by a steel bridge linker. The structures indicated were exposed to three far-field records. Additionally, certain investigations utilized nonlinear time history dynamic analysis. The following are the results:

1. The maximum absolute displacement decreased by 14 % at the level where the linker bridge is placed, particularly in the corner region adjacent to the bridge, in the two tall buildings equipped with end shear walls and linker bridges. This reduction presents that end shear walls effectively control lateral deformation at crucial interface positions where dynamic interaction between the two towers is most substantial as the improves torsional stiffness increases overall lateral resistance and minimizes differential movements between the towers. This is particularly significant because excessive differential displacement at the bridge-adjacent level could impair the integrity of the linker bridge connections, leading to potential failure of the coupling mechanism. From a practical perspective, this result suggests that strategic placement of end shear walls in twin-tower configurations with linker bridges can effectively mitigate the risk of excessive drift and resulting damage to bridge connections.
2. Under far-field ground motion records, the average maximum absolute acceleration at the level where the linker bridge is located decreased by 5 % and 10 % in the two tall buildings with end shear walls, respectively, compared to the corresponding buildings without end shear walls. This reduction presents that end shear walls lead to a more controlled dynamic environment by dissipating seismic energy and decreasing acceleration transmission to the bridge-adjacent levels, thereby improving occupant comfort and reducing vibrational stresses on the linker bridge. The differential reduction between the two towers (5 % versus 10 %) suggests that the efficacy of end shear walls may vary depending on the specific dynamic characteristics of each tower, highlighting the importance of considering individual tower behavior in the design of coupled systems.
3. The skewness coefficient resulting with the maximum absolute acceleration record reduced by 65 % and 66 % due to the presence of end shear walls at the level where the linker bridge is situated, while the kurtosis coefficient was reduced by 14 % and 15 % at that same level. These statistical decreases indicate that the acceleration distributions in buildings with end shear walls are more symmetric and less peaked, indicating a more regular and foreseeable dynamic response under seismic excitation. The substantial reduction in skewness shows that the acceleration time series in buildings with end shear walls more closely approximate a normal distribution, showing less directional bias and more uniform response, while the moderate demonstrating in kurtosis suggests fewer extreme acceleration spikes. These findings indicate that the inclusion of end shear walls significantly affected the seismic behavior of the two reinforced concrete buildings with linker bridges by providing a more regular and statistically stable dynamic response at the critical bridge-adjacent level.
4. According to the statistical analysis, the box plot domain of the maximum absolute displacement reduced by 20 % at the level where the linker bridge is located in the two tall buildings equipped with end shear walls and linker bridges. This reduction in data dispersion demonstrates that end shear walls provide more consistent control over lateral displacements, reducing the variability of the structural response and ensuring more predictable performance under seismic loading. The narrower box plot range reflects a more controlled and uniform displacement pattern, which is essential for maintaining the serviceability and safety of the interconnected towers.
5. The detrended normal Q–Q plot data of the maximum absolute acceleration indicated a 20 % reduction due to the presence of end shear walls in the two tall buildings equipped with both end shear walls and linker bridges, specifically at the level where the linker bridge is situated. This improvement in normality shows that end shear walls contribute to a more regular and statistically stable acceleration response, reducing the likelihood of extreme deviations from the expected behavior and enhancing the reliability of the structural system under seismic excitation. This statistical regularity is particularly important for the linker bridge, as it implies more predictable relative movements between the two towers, reducing the risk of unanticipated stresses or connection failures. The measured decrease confirms that end shear walls provide a stabilizing effect on the dynamic response at the critical bridge-adjacent level.
6. The column force reduced by 69 % and 77 % at the points where the linker bridge is positioned in the two tall buildings incorporating with both end shear walls and linker bridges, specifically at the level adjacent to the bridge. This substantial reduction presents that end shear walls effectively redirect seismic forces away from critical vertical members at the bridge connection points, significantly decreasing the risk of column imbalance, buckling, or failure under extreme loading

conditions. The dramatic reduction underscores the crucial role of end shear walls in protecting the load path at the most vulnerable locations.

It should be noted that the present study is limited to two specific 30-story building configurations connected by a steel linker bridge at a single level, subjected to only three far-field earthquake records, and analyzed with fixed joint and roller support conditions. Therefore, the findings may not be directly generalizable to buildings of varying heights, bridges at different levels, other support types, or near-field ground motions. Future studies are recommended to explore a greater range of parameters to establish more comprehensive design guidelines.

Overall, the results clearly indicate that incorporating end shear walls in tall reinforced concrete buildings connected by linker bridges leads to substantial improvements in seismic performance. The observed reductions in displacement, acceleration, statistical dispersion, and column force, particularly at the floor level adjacent to the linker bridge, highlight the effectiveness of end shear walls in increasing structural stability under far-field ground motion records. These findings underscore the importance of strategic shear wall placement in mitigating seismic demands and optimizing dynamic response in high-rise systems with interconnecting elements.

References

1. Akhavan Salmassi, M., Kheyroddin, A., Hemmati, A. Seismic Behavior of Tall Buildings with End Shear Walls and Opening. Journal of Seismology and Earthquake Engineering. 2021. 23(2). Pp. 55–70. DOI: 10.48303/jsee.2023.1973892.1036
2. Kontoni, D.P.N., Akhavan Salmassi, M. Effect of end shear walls on seismic pounding between two adjacent reinforced concrete high-rise buildings. Asian Journal of Civil Engineering. 2025. 26. Pp. 4649–4664. DOI: 10.1007/s42107-025-01448-y
3. Tambunan, M.L.S., Sjah, J., Rarasati, A.D., Sulistian, R., Trigunarsyah, B. Optimizing Seismic Design of Multi-Tower Buildings Using Sky Bridge Isolation and BIM: A Case Study. International Journal of Engineering & Technology Innovation. 2024. 14(4). Pp. 355–377. DOI: 10.46604/ijeti.2024.13409
4. Arada, A.H., Ozturk, B., Kassem, M.M., Nazri, F.M., Tan, C.G. Optimization of Sky-Bridge location at coupled high-rise buildings considering seismic vulnerability functions. Structural Engineering and Mechanics. 2022. 82(3). Pp. 385–400. DOI: DOI: 10.12989/sem.2022.82.3.385
5. Abbood, I.S., Mahmod, M., Hanoon, A.N., Jaafar, M.S., Mussa, M.H. Seismic response analysis of linked twin tall buildings with structural coupling. International Journal of Civil Engineering and Technology. 2018. 9(11). Pp. 208–219.
6. Saeed, A., Najm, H.M., Hassan, A., Qaidi, S., Sabri, M.M.S., Mashaan, N. S. A Comprehensive Study on the Effect of Regular and Staggered Openings on the Seismic Performance of Shear Walls. Buildings. 2022. 12(9). Article no. 1293. DOI: 10.3390/buildings12091293
7. Abaev, Z.K., Sanakoev, S.G., Dzampaev, O.K., Valiev, A.D. Dynamic characteristics and response of buildings of different structural types and configurations. Construction of Unique Buildings and Structures. 2025. 4(118). Article no. 11804. DOI: 10.4123/CUBS.118.4
8. Chan, C.M. Optimal lateral stiffness design of tall buildings of mixed steel and concrete construction. The Structural Design of Tall Buildings. 2001. 10(3). Pp. 155–177. DOI: 10.1002/tal.170
9. Penumatcha, K.R., Vipparthy, R., Yadav, A. A Study on Effect of Connecting Beams in a Twin Tower Structure. Journal of The Institution of Engineers (India): Series A. 2020. 101. Pp. 847–856. DOI: 10.1007/s40030-020-00482-0
10. Meng, F., Ruan, X., Zhao, J., Qiu, J., Meng, L., Hou, P. Analysis of horizontal vibration characteristics of unequal height twin towers of rigid connected structure. Journal of Building Engineering. 2022. 50. Article no. 104146. DOI: 10.1016/j.jobe.2022.104146
11. Nagar, S., Maru, S. Seismic Analysis of Twin Tower Structures. A Review. International Journal for Research in Applied Science and Engineering Technology. 2021. 9(7). Article no. 36935. DOI: 10.22214/ijraset.2021.36935
12. Ezra, M., Rynkovskaya, M.I., Dereje, L.S., Baza, T.T. Structural dynamics of systems under dynamic loads. A review. AlfaBuild. 2025. 34(2(34)). Article no. 3402. DOI: 10.57728/ALF.34.2
13. Kamran, Ahmad S., Khan, R.A. 2022. Seismic behavior of heritage building with isotropic and orthotropic material properties. a comparative analysis. Materials Physics and Mechanics. 48(3). Pp. 428–442. DOI: 10.18149/MPM.4832022_13
14. Sureshbhai, T.V., Thakkar, J. Behavior of Multi-Storey Twin Structure Connection of The Beams at Different Level: A Mini Review. International Research Journal of Engineering and Technology (IRJET). 10(3). Pp. 121–125.
15. Prajapati, K., Chourasia, M., Scholar, P.G. Analysis of A Tall Twin Tower Considering Lateral Load as Per IS 1893: I: 2016 Using ETABS. International Journal of Scientific Research in Civil Engineering. 2023. 7(1). Pp. 8–21. DOI: 10.32628/IJSRCE22712
16. Pranamika, R., Pandian, D.M.S. Comparison of Twin Towers to Single Tower under Seismic Loading Using E-Tabs. International Journal of Advanced Research in Engineering and Technology (IJARET) Vol. 11(12). Pp. 2790–2809. DOI: 10.34218/IJARET.11.12.2020.262
17. Shinde, P., Sonawane, S., Chandanshive, V. Seismic Resilience, Sustainability, and Torsional Performance of Asymmetric Twin-Tower High-Rise Structures in Seismic Zone V. 2026 International Conference on Communication, Computing and Emerging Technologies (IC3ET). Vasai, 2026. Pp. 1207–1211. DOI: 10.1109/IC3ET64989.2026.11467311
18. Morad, M., Rezaei, S., Farzanian, S., Saravi, P.M. The Effect of Using Skybridge and Its Various Design Methods on the Performance of Multitower. Earthquake Engineering and Resilience. 2026. 5(2). Pp. 161–179. DOI: 10.1002/eer2.70041
19. ETABS® Version 2015. Integrated Software for Structural Analysis and Design of Buildings. Computers and Structures, Inc. Walnut Creek, CA & New York, NY, USA. 2015. URL: https://www.csiamerica.com/products/etabs (date of application: 05.11.2025).
20. Zhu, T.J., Heidebrecht, A.C., Tso, W.K. Effect of peak ground acceleration to velocity ratio on ductility demand of inelastic systems. Earthquake engineering & structural dynamics. 1988. 16(1). Pp. 63–79. DOI: 10.1002/eqe.4290160106

21. Seismosoft. SeismoSignal – Earthquake Software for Signal Processing of Strong-Motion Data. Seismosoft, 2024. URL: www.seismosoft.com (date of application: 05.11.2025).
22. IBM Corp. IBM SPSS Statistics for Windows (Version 27.0). IBM Corp., 2020. URL: https://www.ibm.com/support/pages/downloading-ibm-spss-statistics-27 (date of application: 05.11.2025).

Information about the authors:

***Mohanad Sabri**, PhD in Technical Sciences*
E-mail: mohanad.m.sabri@gmail.com

***Mehran Akhavan Salmassi**, PhD in Structural Engineering*
ORCID: https://orcid.org/0000-0002-9850-6565
E-mail: m.akhavansalmassi@iau.ir

Received 06.11.2025. Approved after reviewing 02.06.2026. Accepted 03.06.2026.